Effect of the atmospheric conditions on wireless optical communication in both 785 nm and 1550 nm

TAREK JIHAD MADI[1], YAHIA ELBASHAR[2*], BASSAM GHAZOLIN[1]

[1] Department of Physics, Faculty of science, Tishreen University, Syria
[2] Department of Basic Science, ELGazeera High institute for Engineering and Technology, Cairo, Egypt
*Corresponding author: Yahia Elbashar y_elbashar@yahoo.com

Abstract

This work aims to enhance the performance of wireless optical communication in the near infrared band by studying the effect of atmospheric factors and tropospheric fluctuations on the propagation of laser light. A physical comparison between laser in the range of wavelength of 785 and 1550 nm respectively is inclusive, in order to select the appropriated link that withstand such weather fluctuations.

Keywords: Wireless optical communication, Laser attenuation – BER law – Quality factor, channel absorption and scattering loss, LED.

Introduction

Many factors can limit the capabilities of the mobile traditional radio communications, such as channel width, capacity, transmission rate, and frequency range. Consequently, traditional radio communications are facing many difficulties to meet the increased requirements for high transmission rates and numerous services. Moreover, this step, studies and find the alternative solutions and techniques such as coding-smart antennas-and multiple input and output" MIMO" systems [1-6].

Achieving 10, Gbps high data rates using radio systems is difficult. According to Cisco, the usage of the Internet is expected to increase 27 times during the period between 2016 and 2021 [7-14]. It is expected that there will be increased growing demand for data rate, whereas the radio waves is used and planned for systems at near future, as 5G cellular systems [15-20]. Therefore, telecommunications system operators competed the other systems to produce high-speed "wireless communication systems" to clients, such as wireless optical communication systems and millimeter-wave wireless communications, as Figure 1 shows a portion of the electromagnetic spectrum that contains optical frequencies, which include infrared, visible light and ultraviolet rays [20-34]. In addition, it contains millimeter waves, which extend within the frequency range 30-300 GHz.

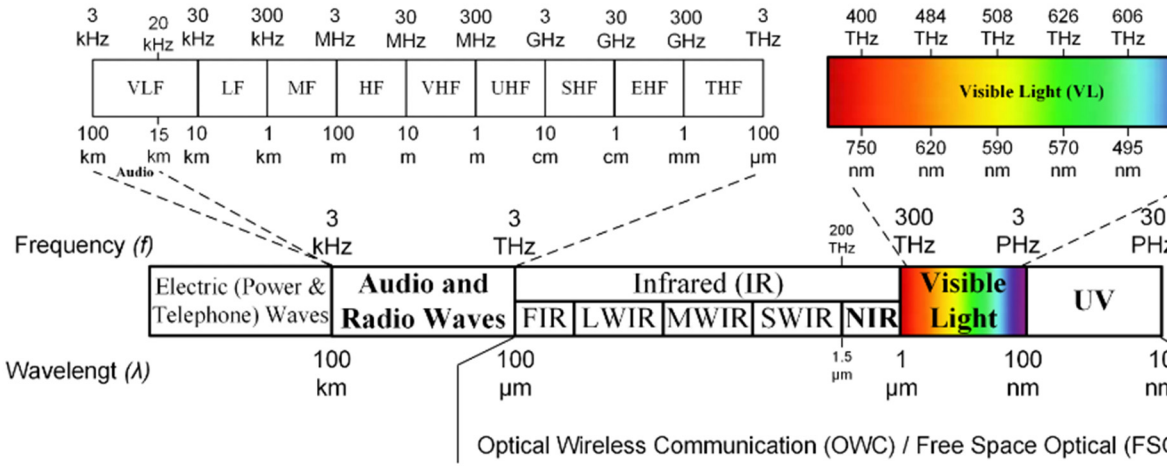

Figure 1: Electromagnetic spectrum

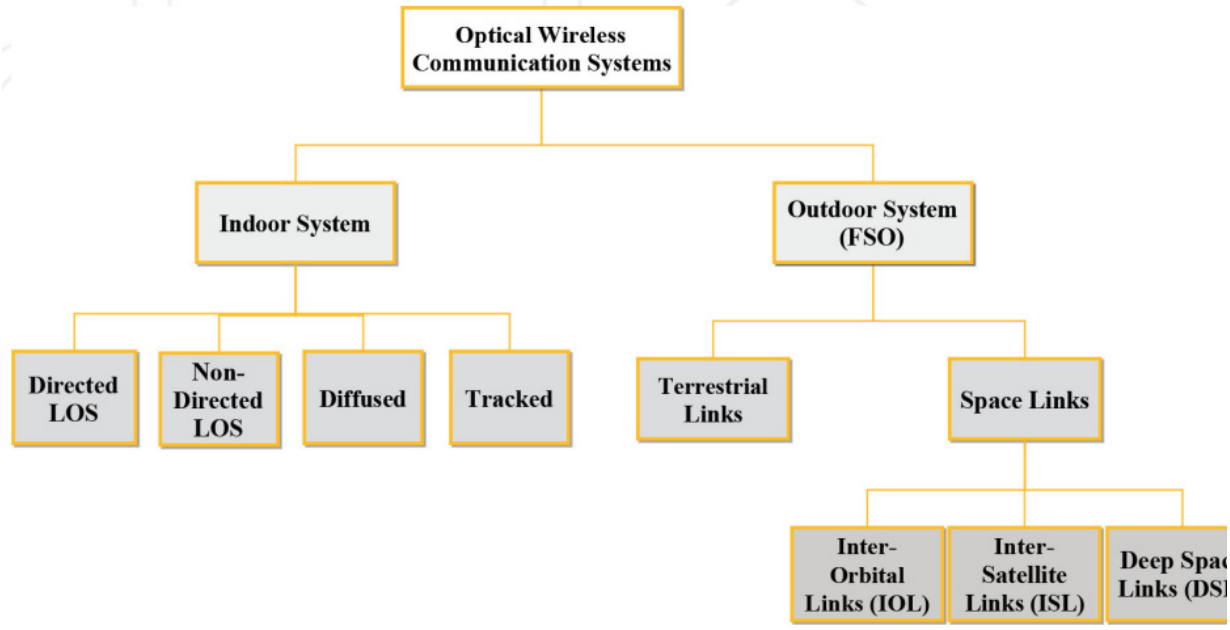

Figure 2: Optical wireless communications types

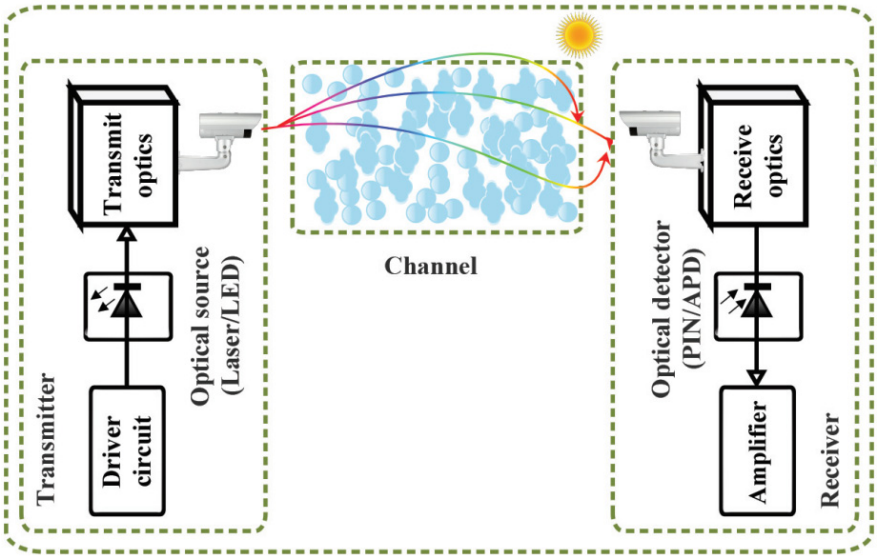

Figure 3: A schematic of a terrestrial OWC system

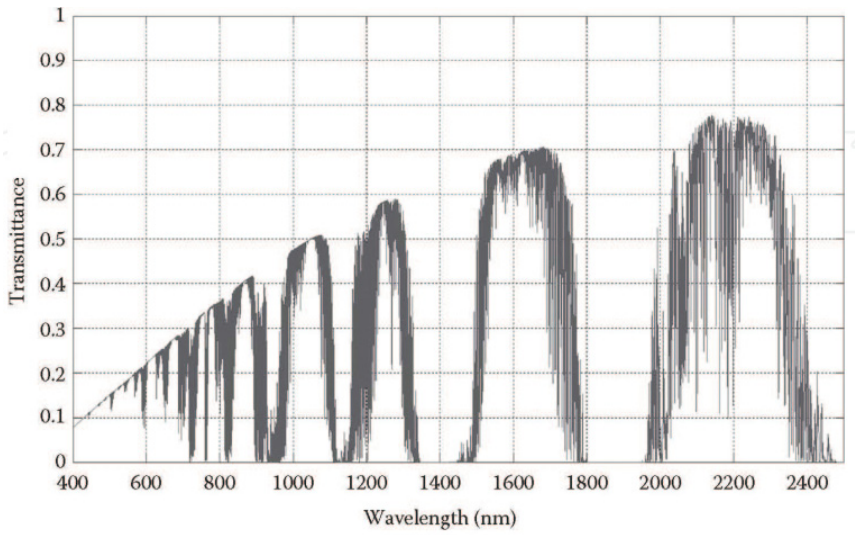

Figure 4: Atmospheric transmittance window with absorption contribution

Where, we notice that millimeter waves are located side by side with light waves and thus share the characteristics of propagation with them, but they are often seen as different, and the most prominent difference between them is that wireless optical communications have benefited from advanced technologies in optical fiber communications, but the equipment that supports millimeter wave communication It is still very much evolving and modern. However, they offer a wide bandwidth and this is the reason for their entry into the 5G networks, where optical wireless communication systems are considered candidates for high data rates to connect between users and the access network. Although work began on the development and implementation of this technology.

An alternative way was used many decades ago to reinforce high-speed data instead of the systems of radio communication, this technique was not famous until the transmitter and receiver components became available with low cost. The rate of dependence on this

technology is expected to increase due to the development of techniques for manufacturing light sources using semiconductors [1][2].

Classification of optical wireless communications

Optical wireless communications are classified in terms of the transmission range into two main categories:[1]

- Indoor OWC
- Outdoor OWC

Figure 2 shows the classification scheme for optical wireless communications, where the indoor wireless optical communications are divided into four types: Direct LOS, Non Direct LOS, Diffused, and Tracked. Whereas, external wireless optical communications are divided into terrestrial optical communications (Terrestrial Link) and satellite optical communications (Space Link).

Block scheme of OWC system

Figure 3 shows an earthen OWC system has (transmitter- channel- and receiver). Transmitter produced waveforms' data which are modulated by an optical carrier. The optical field is generated the radiated through atmospheric channel to the destination. The collected optical field of the receiver is transformed to an electrical current. The transmitted original data can be recovered by processing the detected electrical current, and these data may not be an exact replica of the transmitted original data due to transmission loss that was happened over the channel by the signal. [1] The transmission loss is caused by the effects of the scattering and absorption that are resulted from the molecular constituents and aerosols over the path of transmission.

The base of the atmospheric attenuation absorption is a factor of wavelength and wavelength selective, figure 4 shows the absorption spectra of the atmospheric molecules which is a range of wavelength windows that suffer from minimal absorption compared to other wavelength windows.

Generally the wavelength windows' range is between 780-850 nm and 1520-1600 nm which used in the current OWC equipment are located in the transmission atmospheric windows where molecular absorption is negligible. This leads to mitigate the losses of atmospheric absorption.

Also, certain wavelength windows that are located in the region of four detected wavelengths such as 850, 1060, 1250, and 1550 nm suffer from an attenuation of less than 0.2 dB/km. The 850- and 1550 nm transmission windows coincide with that of standard transmission for fiber communication systems.[3]

Optical transmitter

The optical transmitter consists of two main parts: the optical source and the optical modulator.

Optical source

The light source supplies the information-carrying optical signal that will propagate through the optical channel, as it converts electrical energy into an optical signal of a certain frequency, while providing sufficient power to overcome the damping that occurs to the optical signal during its propagation to reach the receiving end with a power level higher than

the sensitivity of the receiver. The light source in the optical communication system corresponds to the local oscillator or the frequency component responsible for securing the carrier frequency signal in radio and microwave communication systems [4] [5].

The laser beam has the following properties:

1. Monochromatic, that is, all photons have the same frequency.

2. Associated with phase, that is, all the photons produced by the excited emission have the phase of the photon that is induced.

3. The diffraction of the laser beam is small, that is, the beam section does not expand much (unlike radiating diodes) when moving away from the laser source.

Modulation

The goal of modulating the signal is to change one of the characteristics of the optical signal (amplitude - frequency - phase) in proportion to the series of bits expressing the information to be transmitted, and thus the signal expressing the information transforms from its electrical form (bit series) to its optical form (modified light source signal) [4] [5].

Free-Space Optical Channel

The atmospheric channel contains multiple gases and very small particles as (aerosols-dust-smoke..etc) and big particles as (rain-haze-snow-fog), these atmospheric constituents caused the reduction of power level and attenuation of optical signal according to several functions, also absorption of light b gas molecules, Rayleigh, or Mie scattering.

Absorption and scattering loss

While laser beam is spreading through the atmosphere of the Earth, it will interact with many gas molecules and aerosols particles are in the atmosphere. Absorption is responsible for the loss in the atmospheric channel and (Beer's law) describes the process of scattering. The basic atmospheric absorbers at (IR and visible wavelengths) are (water-carbon dioxide and Ozone). The atmospheric absorption is a (wavelength-dependent phenomenon).

The wavelength range of the FSO communication system's wavelength is detected to have "minimal absorption". This is called (atmospheric transmission window). In this window, the attenuation according to molecular or aerosol absorption is less than (0.2 dB/km). There are various windows of transmission their range is (700 – 1600) nm. Majority of FSO systems are intended to operate in the windows of (780 – 850) nm and 1520 - 1600 nm. These wavelengths have been detected because of the readily availability of the transmitter and detector components at these wavelengths. The wavelength depend on attenuation under different weather conditions is commonly available in databases such as (MORTRAN, LOWTRAN and HITRAN).

Scattering of light is also responsible for degrading the performance of the FSO system. Such as "absorption", scattering is also strongly wavelength dependent. If the size of the particles atmospheric is small comparing to the optical wavelength, then Rayleigh scattering is generated. This scattering is quite prominent for FSO communication around visible or ultraviolet range i.e., wavelengths below 1 μm. However, it can be neglected at longer wavelengths near IR range. Particles such as air molecules and haze cause Rayleigh scattering. If the atmospheric particles size is comparable with the optical wavelength, then

Mie scattering is generated. It is dominant near IR wavelength range or longer. Aerosol particles, fog and haze are major contributors of Mie scattering. The atmospheric particles are larger than the optical wavelength such as rain, snow and hail, so the geometrical optic model describes the scattering better.

The "total atmospheric attenuation" is represented by the atmospheric attenuation coefficient, γ that is a combination of "absorption" and "scattering of light". It is expressed as sum of four individual parameters given as[6]:

$$\gamma = \alpha m + \alpha a + \beta m + \beta a \qquad (1)$$

αm and αa are the absorption coefficients of molecular and aerosol, respectively and βm and βa are the scattering coefficients of molecular and aerosol, respectively.

Fog, Rain and Snow effects

Absorption and scattering in FSO system are caused by several factors as follows:

Fog: The atmospheric attenuation's major contribution is according to fog, which causes of both scattering and absorption. When the visibility is less than 50 m throughout the conditions of dense fog, the attenuation could be more than 350 dB/km and this obviously could limit FSO link availability. The improvement of the chances of link availability could be by specific mitigation techniques. In general, (1550 nm) lasers are a" preferred choice" during heavy attenuation because of their high-transmitted power. Fog can extend vertically up to the height of (400 m) above the Earth's surface. The attenuation according to fog can be predicted by depending on "Mie scattering theory". However, it involves complex computations and requires detailed information of fog parameters. Visibility range information is an alternative approach, in which the attenuation according to fog is predicted using common experimental models. The wavelength of 550 nm is usually taken as the visibility range reference wavelength. Following Eq. defines the detected attenuation of fog given by common experimental model for Mie scattering:

$$\beta_{fog}(\lambda) = \frac{3.91}{V}\left(\frac{\lambda}{550}\right)^{-p} \qquad (2)$$

V (km) is the visibility range; λ (nm) is the wavelength operating and p the size distribution coefficient of scattering. Kim or Kruse model determine p value.

Rain: has less effect than fog because of the size of rain droplets, which are larger (100 to 1000 μm) than the wavelength, which used at FSO communication.

The attenuation loss ranges from 1 dB/km to 10 dB/km for (850nm-1500nm) wavelength whereas the light rain attenuation loss is (2.5 nm/hr) and heavy rain attenuation loss is (25 mm/hr). Detected attenuation, αrain (in) for a FSO link is given by:

$$\alpha_{rain} = k_1 R^{k_2} \qquad (3)$$

R: is the rain rate, which is measured in mm/hr.

K1,K2: parameters models which their values are connected with raindrops' size and the temperature of rain, it can be realized that low clouds result a very high attenuation so it's better to use high power lasers which is must be greater than 300 dB at FSO system.

Snow: The attenuation of snow is more than rain but also less than fog due to that snowflakes are between (fog and rain). Laser beams' path is blocked when snowflakes' density increases, so the attenuation's range is between 30-350 dB/km and due to this significantly reduces the link availability of the FSO system. For snow, attenuation is classified into dry and wet snow attenuation. The specific attenuation (dB/km), αsnow for snow rate S in mm/hr is given as:

$$\alpha_{snow} = aS^b \qquad (4)$$

Where: the parameters values a , b at dry and wet snow conditions:

$$Dry\ snow:\ a = 5.42 \times 10^{-5} + 5.49;\ b = 1.38 \quad (5)$$

$$Wet\ snow:\ a = 1.05 \times 10^{-4} + 3.78;\ b = 0.72 \quad (6)$$

Results and Discussion

We perform the simulation for external modulation using the MZ modulator and an APD photodetector. And we change both the channel length and the channel attenuation factor - as the total attenuation of the channel is equal to the product of the channel length by the attenuation factor - for the wavelengths used in the transmission windows, which were studied in the theoretical section: 785 and 1550 nm.

The simulation is carried out in two stages: in the first we fix the attenuation factor and change the length of the wireless channel, and in the second we fix the length of the wireless channel and change the attenuation factor, in order to determine the maximum total attenuation of the channel at which the link operates with acceptable performance. However, the performance is considered acceptable for bit-error rate values of 10^{-9} and lower and for a quality factor of 6 and more [7-9].

Performance evaluation of the 785 nm wavelength

The first stage: The attenuation factor is fixed to the value 5 dB/Km and the channel length is changed within the range 10-12 Km. The evaluate both the bit-error rate and the quality factor, so we get Table 1.

We can see from Table 2 that the performance declines with the increase in the communication distance due to the increase in the total attenuation of the channel. We also note that for a communication distance of 11.6 km, the quality factor is 6.30 and the rate of bit error of the 10^{-11} order It is acceptable, but for a greater connection distance, the performance decreases. Figure 5 shows an eye diagram for different connection distances.

We can see from the diagrams in Figure 5 that the performance declines with increasing total attenuation due to the increase in channel length, and that the eye aperture becomes smaller as bit level "1" approaches bit level "0" and it is difficult to distinguish between them. We conclude that for an attenuation factor of 5 dB/Km the wavelength of 785 nm is limited by a communication distance of 11.6 Km. That is, limited to a total attenuation of the order of 58 dB.

The second stage: the channel length is fixed to the value 2 Km and the attenuation coefficient is changed within the range 31-34 dB/Km. We evaluate both the bit-error rate and the quality factor, so we get Table 3.

We can see from Table 3 that the performance decreases when the channel attenuation factor increases due to the increase in the total channel attenuation, and we also note that for the attenuation factor 36.6 dB/km the quality factor is 6.46 and the rate of bit error is of the of 10^{-11}order, Which is an acceptable performance, but for larger values of the channel

attenuation factor the performance declines. Figure 6 shows an eye diagram for different attenuation coefficient values.

We can see from the diagrams in Figure 6 that the performance declines with the increase of the total attenuation due to the increase in the channel attenuation factor, and that the eye aperture becomes smaller as the bit level "1" approaches the bit level "0" and it is difficult to distinguish between them. We conclude that when the length of channel is 2 kmm the 785 nm wavelength is limited by a channel attenuation coefficient of 36.6 dB/Km, that is, limited by a total attenuation of the order of 73.2 dB We also note that there is a difference between the total attenuation in the first stage (variable large channel length and constant channel attenuation factor) and the total attenuation in the second stage (constant small channel length and variable attenuation factor) in which the performance is at the minimum acceptable limits, for the same reason which is path loss The free signal when it travels through the channel and it increases with the length of the channel.

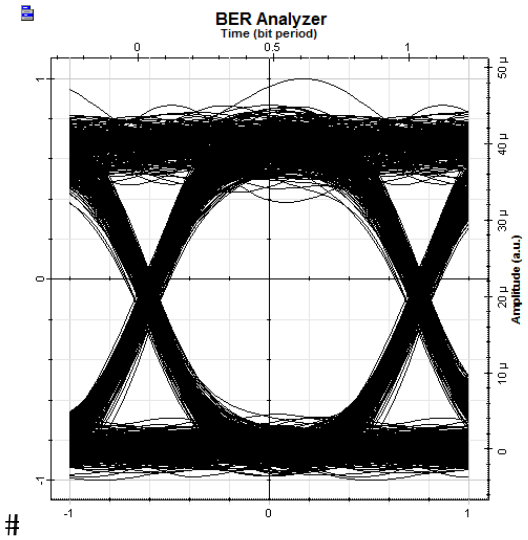

#

#Figure 5-b: 11 Km

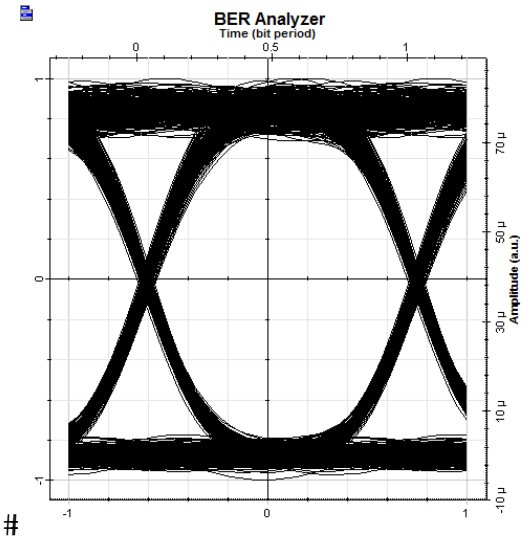

#

#Figure 5-a: 10.5 Km

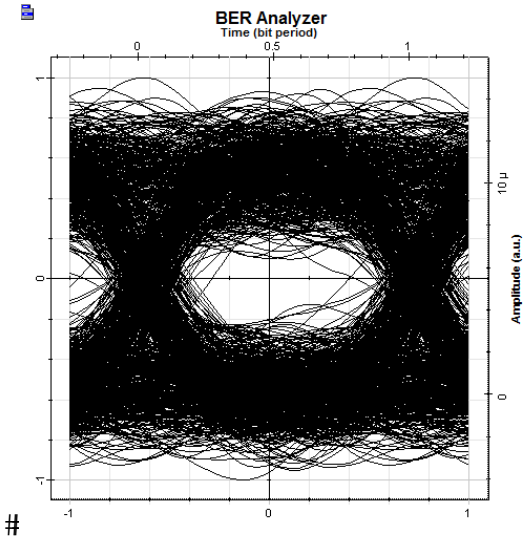

#

#Figure 5-d: 12 Km

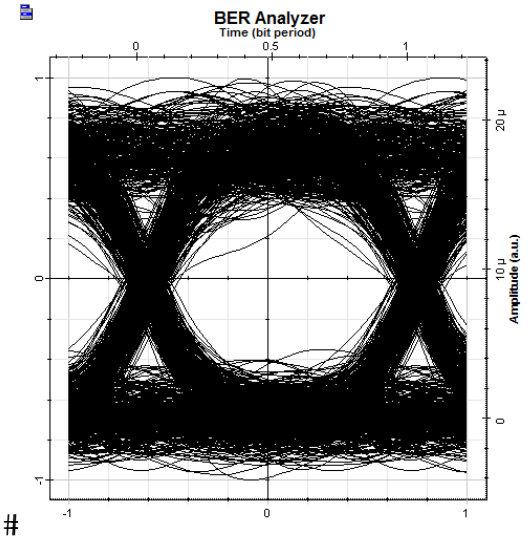

#

#Figure 5-c: 11.6 Km

#Figure 5: an eye diagram for 5 dB/Km and variable channel length ($785nm$)

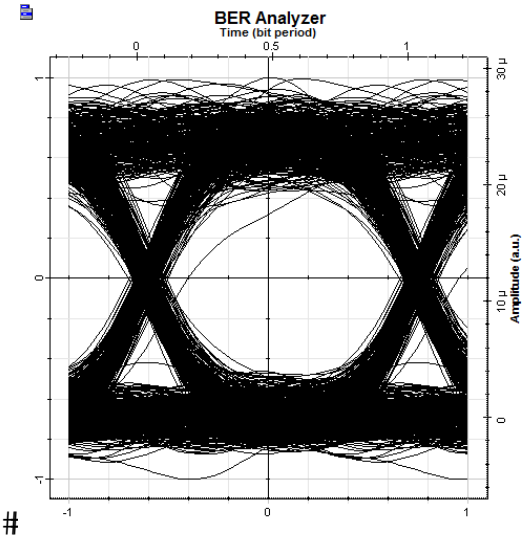

#

#Figure 6-b: 32.4 dB/Km

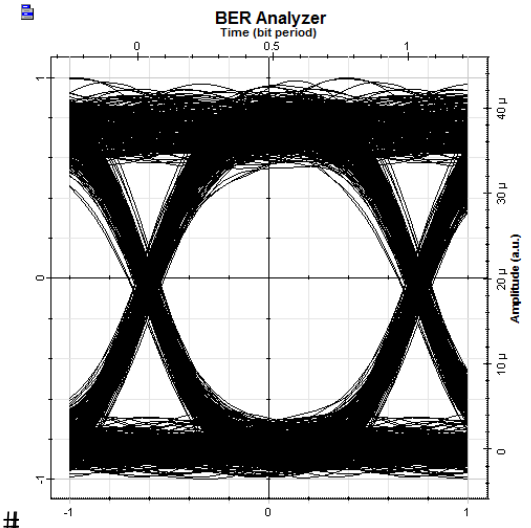

#

#Figure 6-a: 31.6 dB/Km

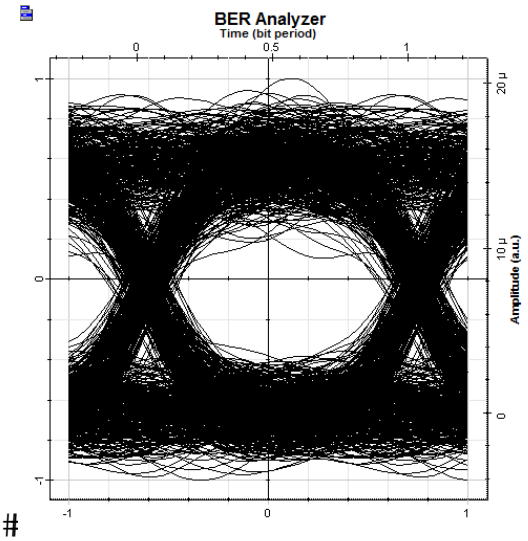

#

#Figure 6-d: 34 dB/Km

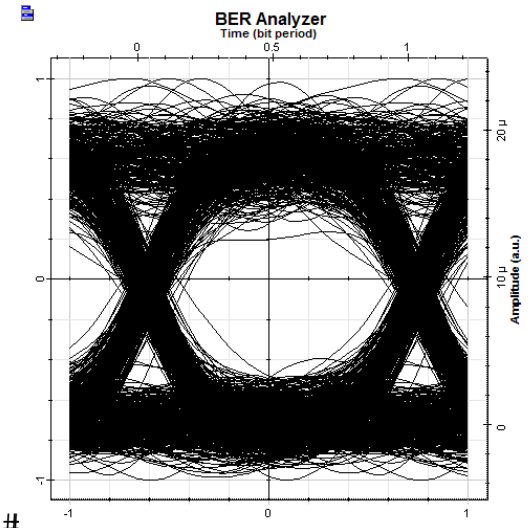

#

#Figure 6-c: 33.2 dB/Km

#Figure 6: an eye diagram for 2 Km and variable attenuation factor ($785nm$)

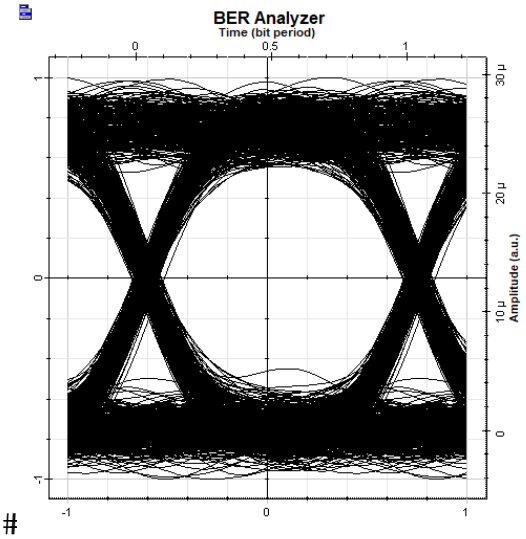

#Figure 7-b: 9.5 Km

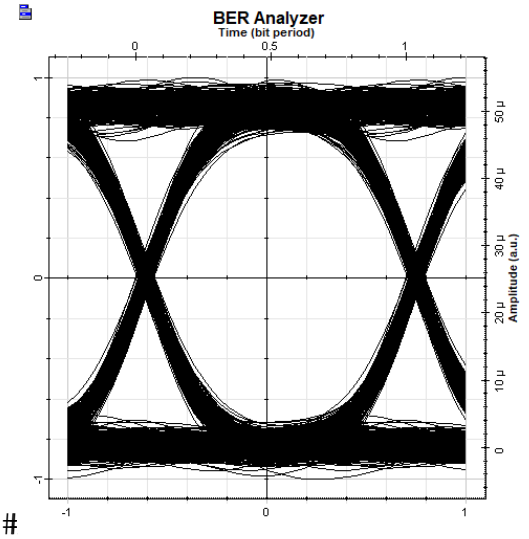

#Figure 7-a: 9 Km

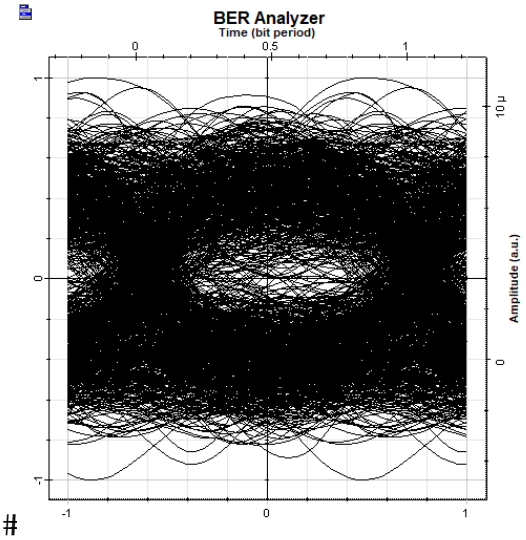

#Figure 7-d: 10.5 Km

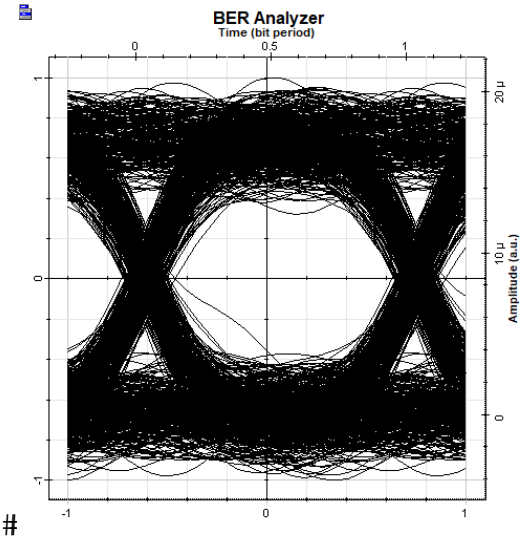

#Figure 7-c: 9.8 Km

#Figure 7: an eye diagram for 5 dB/Km and variable channel length ($1550nm$)

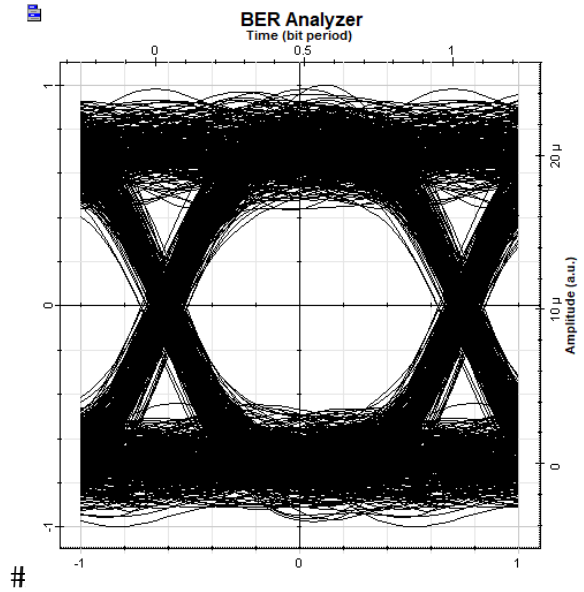

#

#Figure 8-b: 31.8 dB/Km

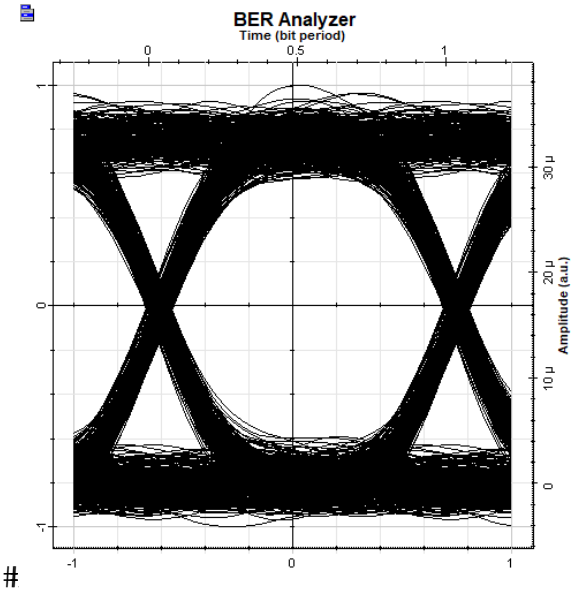

#

#Figure 8-a: 31 dB/Km

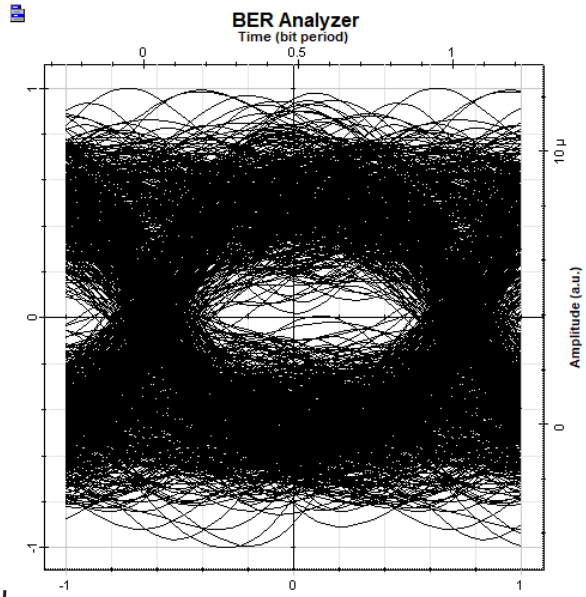

#

#Figure 8-d: 33 dB/Km

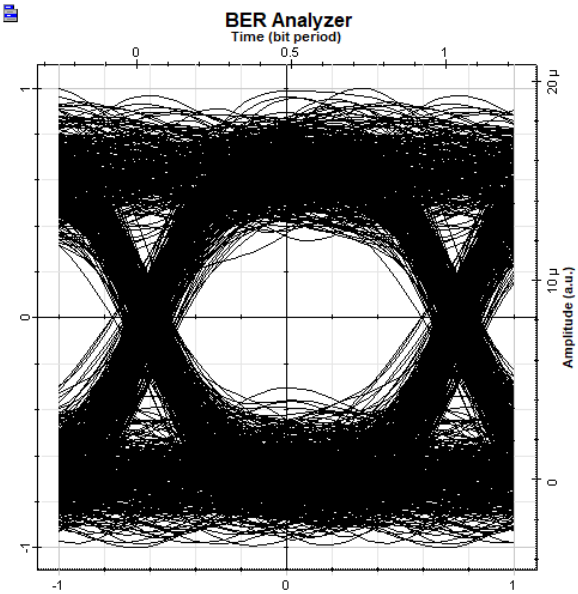

#

#Figure 8-c: 32.4 dB/Km

#Figure 8: an eye diagram for 2 Km and variable attenuation factor (1550 nm)

Table 1 shows a number of typical values of clear weather conditions absorption coefficients of molecular.

Table (1): Molecular absorption at typical wavelength	
Wavelength (nm)	Molecular Absorption (dB/km)
550	0.13
690	0.01
850	0.41
1550	0.01

Table (2): BER and QF for 785 nm and variable channel length

$Length\ (Km)\#$	$Atten.(dB)$	QF	BER
10	50	36.60	10^{-293}
10.1	50.5	32.78	10^{-236}
10.2	51	29.25	10^{-188}
10.3	51.5	27.38	10^{-165}
10.4	52	23.75	10^{-125}
10.5	52.5	21.65	10^{-104}
10.6	53	19.78	10^{-87}
10.7	53.5	18.37	10^{-75}
10.8	54	15.76	10^{-56}
10.9	54.5	14.42	10^{-47}
11	55	12.40	10^{-35}
11.1	55.5	11.42	10^{-30}
11.2	56	10.80	10^{-27}
11.3	56.5	9.20	10^{-20}
11.4	57	7.90	10^{-16}
11.5	57.5	6.90	10^{-12}
11.6	58	6.30	10^{-11}
11.7	58.5	5.66	10^{-9}
11.8	59	5.06	10^{-7}
11.9	59.5	4.58	10^{-6}
12	60	3.5	10^{-5}

Table (3): BER and QF for 785 nm and variable attenuation factor

$\alpha\ (dB/Km)\#$	$Atten.(dB)$	QF	BER
34	68#	17.94	10^{-72}
34.2	68.4#	16.18	10^{-59}
34.4	68.8#	15.09	10^{-52}
34.6	69.2#	13.69	10^{-43}
34.8	69.6#	13.62	10^{-42}
35	70#	12.37	10^{-35}
35.2	70.4#	11.07	10^{-29}
35.4	70.8#	11.04	10^{-28}
35.6	71.2#	9.71	10^{-22}
35.8	71.6#	8.73	10^{-18}
36	72	8.44	10^{-17}
36.2	72.4#	7.35	10^{-14}
36.4	72.8#	6.92	10^{-12}
36.6	73.2#	6.46	10^{-11}
36.8	73.6#	5.80	10^{-9}
37	74#	5.30	10^{-8}

Table (4): BER and QF for 1550 nm and variable channel length

$Length\ (Km)\#$	$Atten.(dB)$	QF	BER
8.5	42.5	36.00	10^{-284}
8.6	43	31.72	10^{-221}
8.7	43.5	29.53	10^{-129}
8.8	44	25.34	10^{-142}
8.9	44.5	22.68	10^{-114}
9	45	19.27	10^{-83}
9.1	45.5	16.65	10^{-62}
9.2	46	14.72	10^{-49}
9.3	46.5	12.53	10^{-36}
9.4	47	11.25	10^{-29}
9.5	47.5	9.98	10^{-24}
9.6	48	8.71	10^{-18}
9.7	48.5	7.61	10^{-14}
9.8	49	6.44	10^{-11}
9.9	49.5	5.64	10^{-9}
10	50	5.1	10^{-7}
10.1	50.5	4.49	10^{-6}
10.2	51	3.9	10^{-5}
10.3	51.5	3.4	0.0003
10.4	52	2.8	0.002
10.5	52.5	–	–

Table (5): BER and QF for 785 nm and variable attenuation factor

$\alpha\ (dB/Km)$	$Atten.(dB)$	$QF\#$	$BER\#$
30	60	12.22#	10^{-34}
30.2	60.4	11.73#	10^{-32}
30.4	60.8	10.11#	10^{-24}
30.6	61.2	9.51#	10^{-22}
30.8	61.6	8.59#	10^{-18}
31	62	8.04#	10^{-16}
31.2	62.4	6.93#	10^{-12}
31.4	62.8	6.5#	10^{-11}
31.6	63.2	6#	10^{-10}
31.8	63.6	5.6#	10^{-8}
32	64	5.1#	10^{-7}
32.2	64.4	4.6#	10^{-6}
32.4	64.8	4.5#	10^{-6}
32.6	65.2	3.9#	10^{-5}
32.8	65.6	3.5#	0.0002
33	66	3.1#	0.0009

Performance evaluation of the 1550 nm wavelength

The first stage: the attenuation parameter is fixed to the value 5 dB/Km and the channel length is changed within the range 8.5-10.5 Km and we evaluate both the bit-error rate and the quality factor, we get Table 4.

We can see from Table 4 that the performance declines with the increase in the communication distance due to the increase in the total attenuation of the channel. It is acceptable, but for a greater connection distance, the performance decreases. Figure 7 shows an eye diagram for different communication distances.

We can see from the diagrams in Figure 7 that the performance deteriorates with the increase in the total attenuation due to the increase in the length of the channel, and that the eye aperture becomes smaller as the "1" bit level approaches the "0" bit level and it is difficult to distinguish between them. We conclude that for the attenuation coefficient of 5 dB/Km the wavelength of 1550 nm is limited by a communication distance of 9.8 Km. That is, limited to a total attenuation of the order of 49 dB.
The second stage: The channel length is fixed to the value 2 Km and the attenuation coefficient is changed within the range 30-33 dB/Km. We evaluate both the bit-error rate and the quality factor, so we get Table 5.

We can see from Table 5 that the performance declines with the increase in the channel attenuation factor due to the increase in the total channel attenuation, and we also note that for the attenuation factor 31.6 dB/km the quality factor is 6 and the rate of bit-error is of the of 10^{-10} order which is an acceptable performance, but for larger values of the channel attenuation coefficient the performance declines.

Figure 8 shows an eye diagram for different attenuation coefficient values.

We can see from the diagrams in Figure 8 that the performance deteriorates as the total attenuation increases due to the increase in the channel attenuation factor, and that the eye aperture becomes smaller as the bit level “1” approaches the bit level “0” and it is difficult to distinguish between them. We conclude that in case of the length of channel is 2 km , the wavelength of (1550 nm) is limited by a channel attenuation coefficient of 31.6 dB/Km, that is, limited by a total attenuation of the order of 63.2 dB Here, too, we note that there is a difference between the total attenuation in the first stage and the total attenuation in the second stage, due to the loss of the free path of the signal when it travels through the channel and it increases with increasing the length of the channel

Conclusions

We compare the wavelengths with each other for the minimum acceptable performance. The wavelength 785 nm and 1550 nm were studied the max absorbance in the 2Km was 36.6 and 31.6 dB/Km with Attenuation 73.2 and 63.2 dB respectively. The channel length for 5dB/Km was 11.6Km and 9.8Km with attenuation 58 and 49 dB respectively.

There is a difference in the damping coefficient for the order of 5 dB/Km between the two wavelengths 785-1550 nm and a difference in the channel length of the order of 1.8 Km between the two wavelengths 785-1550 nm, so it is preferable to use the wavelength of 785 nm.

References

[1] Alimi, I., Shahpari, A., Sousa, A., Ferreira, R., Monteiro, P., & Teixeira, A. Challenges and opportunities of optical wireless communication technologies. Optical communication technology, (2017)

[2] Arun K. Majumdar, Jennifer C. Ricklin, “Free-Space Laser Communications Principles and Advances”, Springer (2008)

[3] Alkholidi, Abdulsalam Ghalib, and Khaleel Saeed Altowij. "Free space optical communications—Theory and practices." Contemporary Issues in Wireless Communications: 159-212. (2014)

[4] John M. Senior, “Optical Fiber Communications Principles and Practice, Third Edition”, (2009)

[5] M. N. O. Sadiku, S.M. Musa, “Free Space Optical Communications: An Overview”, European Scientific Journal, vol.12, No.9, 55-68 (2016)

[6] Hemani Kaushal, V.K. Jain, Subrat Kar, “Free Space Optical Communication”, Springer (2017)

[7] M. H. M. Shamim, M. A. Shemis, M. Z. M. Khan, Analysis of optical injection on red and blue laser diodes for high bit-rate visible light communication, Optics Communications, Volume 449, Pages 79-85 (2019)

[8] Basudeb Das, Shibabrata Mukherjee, Saswati Mazumdar, Design of a 10 GHz optical wireless communication link using low power C-band laser diode, Results in Optics, Volume 5, 100129 (2021)

[9] Khaleda Mallick, Rinki Atta, Ardhendu Sekhar Patra, Performance evaluation of free space optics communication system in the scenario of triple play service using probabilistic shaping scheme, Optics Communications, Volume 522, 128699, (2022)

[10] Zilan Pan, Yin Xiao, Wen Chen, "Accurate optical information transmission through thick tissues using zero-frequency modulation and single-pixel detection", Optics and Lasers in Engineering, Volume 158, 107133 (2022)

[11] Abu Jahid, Mohammed H. Alsharif, Trevor J. Hall, "A contemporary survey on free space optical communication: Potentials, technical challenges, recent advances and research direction", Journal of Network and Computer Applications, Volume 200, 103311 (2022)

[12] Ao, Jun, Yun Zhi Xia, Long Che, Tao Zhang, and Chun Bo Ma. "Study on Fog Attenuation Characteristics and Experiment Measurement for Laser Propagation in Atmosphere." In Advanced Materials Research, vol. 760, pp. 199-203 (2013)

[13] Kim, Isaac I., Bruce McArthur, and Eric J. Korevaar, "Comparison of laser beam propagation at 785 nm and 1550 nm in fog and haze for optical wireless communications." In Optical wireless communications III, International Society for Optics and Photonics, vol. 4214, pp. 26-37. (2001)

[14] Kwiecień, Janusz. "The effects of atmospheric turbulence on laser beam propagation in a closed space - An analytic and experimental approach." Optics Communications, 433: 200-208, (2019)

[15] Y.H. Elbashar, M.A. Mohamed, A.M Badr, H.A. Elshaikh, Diaa A.Rayan, "X-ray Spectroscopic analysis of nanocrystal phase growth in Cobalt oxide Doped copper zinc sodium phosphate glass matrix", Journal of Optics, 50, pages 253–256 (2021)

[16] Y.H. Elbashar, M.A. Mohamed, D.Rayan, A.M. Badr, and H.A. Elshaikh, "Optical Spectroscopic analysis of bandpass filter used for laser protection based on cobalt phosphate glass", Journal of Optics , Volume 49, Issue 2, 270–276 (2020)

[17] Y.H. Elbashar, Diaa. Rayan, Shimaa.G.El Gabaly, A.A. Mohamed, "Optical spectroscopic study of cobalt oxide doped boron glass and its ion effect on optical properties", Egyptian Journal of Chemistry Volume 63, Issue 6, Page 2111-2124 (2020)

[18] Y. H. Elbashar, R.A. Ibrahem, Jamal Khaliel, S.M. Hussien, A.E. Omran, W.A. Rashidy, M.A. Mohamed, A. S. Abdel-Rahaman, H.H. Hassan," Infrared spectroscopy analysis of vanadium oxide doped sodium zinc phosphate glass matrix", Journal of Nonlinear Optics and Quantum optics, NLOQO Volume 54, Number 3-4, p. 231-239 (2021)

[19] Y. H. Elbashar, W. A. Rashidy, Jamal Khaliel, S.M. Hussien, A.E.Omran, R.A.Ibrahem, M.A. Mohamed, A. S. Abdel-Rahaman, H.H.Hassan, "Molecular Spectroscopic analysis of Sodium phosphate zinc cupper glass matrix doped magnesium", Journal of Nonlinear Optics and Quantum optics, NLOQO Volume 54, Number 3-4, p. 205-215 (2021)

[20] D. Rayan, Y.H. Elbashar, A.M. Abdelghany, "Impact of zinc ions on the physical properties of sodium barium phosphate glass containing Cu2+ ions", Journal of Nonlinear optics and quantum optics, NLOQO Volume 54, Number 3-4, p. 217-229 (2021)

[21] Yahia.H. Elbashar, D. A. Rayan, Hedra Emad R. Saleh, Roshdy A. Abdel Rassoul, "GLASS TECHNOLOGY AND ITS APPLICATION IN SOLAR CELLS", Journal of nonlinear optics and quantum optics, NLOQO Volume 53, Number 3-4, 177-207 (2021)

[22] Y.H. Elbashar, S.M. Hussien, Jamal Khaliel, M.A. Mohamed, A.E.Omran, R.A. Ibrahem, W.A. Rashidy, A.S. Abdel Rahaman, H. H. Hassan , "Infrared spectroscopic analysis of cadmium doped sodium zinc phosphate glass matrix", Journal of nonlinear optics and quantum optics, NLOQO Volume 54, Number 1-2, 105-114 (2021)

[23] Mohammed A. Algradee, Y. H. Elbashar, S. Wageh, H.H. Hassan, "Structural Characterizations and Activation Energy of CdS Nanocrystals Embedded in Novel Glass Matrix", Journal of Optics, 50(3):381–394 (2021)

[24] S. S. Moslem, Yahia. H. Elbashar, Diaa. A. Rayan, Hussam. H. Hassan, "Double Bandpass Absorption Glass Filter: A review", Journal of nonlinear optics and quantum optics, NLOQO Volume 53, Number 3-4, 209-273 (2021)

[25] Yahia. H. Elbashar, D. A. Rayan, Hedra Emad R. Saleh, Roshdy A. Abdel Rassoul, " Optical Spectroscopic Analysis of Neodymium Oxide Doped Phosphate Glass Matrix for Solar Energy Applications", Journal of nonlinear optics and quantum optics, NLOQO Volume 53, Number 3-4, 275-289 (2021)

[26] Y. H. Elbashar, Shimaa G. ElGabaly, D. A. Rayan, "FTIR and NIR spectroscopic analyses of Co3O4 doped sodium zinc borate glass matrix", Journal of Optics, 50(4), 559-568, (2021)

[27] Y. H. Elbashar, J. A. Khaliel, Saedah R.Al-mhyawi, “The influence of Sodium ions on the optical properties for active glass laser medium with matrix Nd2O3-B2O3-ZnO”, nonlinear optics and quantum optics, NLOQO Volume 55, Number 1-2, 45-62 (2022)

[28] Y. H. Elbashar, D. A. Rayan, “Optical spectroscopic analysis of CdO doped copper sodium zinc Phosphate Glass matrix for UV solar cell protection applications”, nonlinear optics and quantum optics, NLOQO Volume 55, Number 1-2, 85-102 (2022)

[29] H.S.Ayoub, A.Attia, A.Emara, A. El-Sherif , Y.H. Elbashar, "Ultraviolet laser shadowgraphic system of measuring ev burner flame", Journal of Nonlinear Optics and Quantum optics, NLOQO, Volume 49., Issue1-2, p. 79-90 (2018)

[30] M. Darwiesh, A.F. El-Sherif, H.S.Ayoub, Y.H. El-Sharkawy, M.F. Hassan, Y.H. Elbashar, “Hyperspectral laser imaging of underwater targets”, Journal of Optics, 47(4):553–560, (2018)

[31] H. S. Ayoub, A.F. El-Sherif, H. H. Hassan, S. A. Khairy, Y.H. Elbashar, "Dilatometry of Refractory Metals and Alloys Using Multi- Wavelength Laser Shadowgraphy of Filament Samples", Journal of Nonlinear Optics and Quantum optics, NLOQO, Volume 49. Issue1-2, p. 51-61(2018)

[32] Amr Attia, H.S.Ayoub, Bassam Ghazolin, A.F. El-Sherief, M. El-Gohary, Ahmed Emara, H. Moneib, Y.H.Elbashar, “In-Situ Soot visualization using Low power 405nm laser shadowgraphy for premixed and non-premixed flames”, Annals of the University of Craiova, Physics, Physics AUC, vol. 28, 12-16 (2018)

[33] M. Darwiesh , A.F. El-Sherif , H.S.Ayoub , Y.H. El-sharkawy , M.F. Hassan , Y.H. Elbashar, “Design and implementation of underwater laser imaging test aquarium”, Journal of Optics, volume 48, issue 1, pp145-153 (2019)

[34] Hussam Hassan, Deia Moubarak, Jamal Khaliel, Hany Ayoub, Ahmed Abdel-Rahaman, Sherif Khairy, Tarek El-Rasasi, Yahia Elbashar, “Design and construction of optical laser shadowgraphy system for measuring the internal friction of high elasticity solids”, Journal of Nonlinear Optics and Quantum optics (NLOQO), Volume 48, Number 4, p. 313-320 (2018)